Howard Hughes Medical Institute

Published as: *Science*. 2015 May 29; 348(6238): 1007–1013.

Engram Cells Retain Memory Under Retrograde Amnesia

Tomás J. Ryan[1,2,*], **Dheeraj S. Roy**[1,*], **Michele Pignatelli**[1,*], **Autumn Arons**[1,2], and **Susumu Tonegawa**[1,2,†]

[1]RIKEN-MIT Center for Neural Circuit Genetics at the Picower Institute for Learning and Memory, Department of Biology and Department of Brain and Cognitive Sciences, Massachusetts Institute of Technology, Cambridge, MA 02139, USA

[2]Howard Hughes Medical Institute, Massachusetts Institute of Technology, Cambridge, MA 02139, USA

Abstract

Memory consolidation is the process by which a newly formed and unstable memory transforms into a stable long-term memory. It is unknown whether the process of memory consolidation occurs exclusively by the stabilization of memory engrams. By employing learning-dependent cell labeling, we identified an increase of synaptic strength and dendritic spine density specifically in consolidated memory engram cells. While these properties are lacking in the engram cells under protein synthesis inhibitor-induced amnesia, direct optogenetic activation of these cells results in memory retrieval, and this correlates with the retained engram cell-specific connectivity. We propose that a specific pattern of connectivity of engram cells may be crucial for memory information storage and that strengthened synapses in these cells critically contribute to the memory retrieval process.

Main Text

Memory consolidation is the phenomenon whereby a newly formed memory transitions from a fragile state to a stable, long-term state (1–3). The defining feature of consolidation is a finite time window that begins immediately after learning, during which a memory is susceptible to disruption such as protein synthesis inhibition (4–6), resulting in retrograde amnesia. The stabilization of synaptic potentiation is the dominant cellular model of memory consolidation (7–10) because protein synthesis inhibitors disrupt late-phase long-term potentiation of *in vitro* slice preparations (11–13). Although much is known about the cellular mechanisms of memory consolidation it remains unknown whether these processes occur in memory engram cells. It may be possible to characterize cellular consolidation and empirically separate mnemonic properties in retrograde amnesia by directly probing and manipulating memory engram cells in the brain. The term memory engram originally

†Correspondence to: tonegawa@mit.edu.
*These authors contributed equally to this work.

Supplemental reference: (41)

Data and Materials: pAAV-TRE-ChR2-EYFP, pAAV-TRE-ChR2-mCherry, and pAAV-TRE-mCherry were developed by X.L., in the group of S.T., at the Massachusetts Institute of Technology; therefore, a materials transfer agreement (MTA) is required to obtain these virus plasmids.

referred to the hypothetical learned information stored in the brain, which must be reactivated for recall (14–15). Recently, several groups demonstrated that specific hippocampal cells that are activated during memory encoding are both sufficient (16–18) and necessary (19–20) for driving future recall of a contextual fear memory, and thus represent a component of a distributed memory engram (21). Here, we applied this engram technology to the issue of cellular consolidation and retrograde amnesia.

We employed the previously established method for tagging the hippocampal dentate gyrus (DG) component of a contextual memory engram with mCherry (see Materials and Methods, fig. S1, and (16, 22)). To disrupt consolidation we systemically injected the protein synthesis inhibitor anisomycin (ANI) or saline (SAL) as a control immediately after contextual fear conditioning (CFC) (Fig. 1A). The presynaptic neurons of the entorhinal cortex (EC) were constitutively labeled with ChR2 expressed from an AAV_8-CaMKIIα-ChR2-EYFP virus (Fig. 1B). Voltage clamp recordings of paired engram ($mCherry^+$) and non-engram ($mCherry^-$) DG cells were conducted simultaneously with optogenetic stimulation of $ChR2^+$ perforant path (PP) axons (Fig. 1C, D). $mCherry^+$ cells of the SAL group showed significantly greater synaptic strength than $mCherry^+$ cells of the ANI engram group, but the $mCherry^-$ cells of the SAL and ANI groups were of comparable synaptic strength (Fig. 1E). Calculation of AMPA/NMDA current ratios (23) showed that at 24 hours post-training, $mCherry^+$ engram cells displayed potentiated synapses relative to paired $mCherry^-$ non-engram cells in the SAL group (Fig. 1E). However, no such difference between $mCherry^+$ and $mCherry^-$ was observed in the ANI group. In addition, $mCherry^+$ engram cells of the SAL group showed significantly greater AMPA/NMDA current ratios than $mCherry^+$ engram cells of the ANI group. Analysis of miniature EPSCs of engram and non-engram cells of both SAL and ANI groups showed the same pattern (fig. S2).

We also quantified dendritic spine density for DG engram cells labeled with an AAV_9-TRE-ChR2-EYFP virus. Spine density of $ChR2^+$ cells was significantly higher than corresponding $ChR2^-$ cells in the SAL group (Fig. 1F. fig. S3), but spine densities of $ChR2^+$ and $ChR2^-$ cells of the ANI group were similar (see Materials and Methods). Spine density of $ChR2^+$ cells of the SAL group was significantly higher than that of ANI $ChR2^+$ cells (Fig. 1F), but $ChR2^-$ cells were comparable. This result was confirmed by analysis of the membrane capacitance (fig. S4G). ChR2 expression did not affect intrinsic properties of DG cells *in vitro* (fig. S5A–E). Direct bath application of ANI did not affect intrinsic cellular properties *in vitro* (fig. S5F), although it mildly reduced synaptic currents acutely (fig. S5G–I). Importantly, when anisomycin was injected into c-fos-tTA animals 24 hours post-CFC and engram labeling, engram-cell specific increases in dendritc spine density and synaptic strength were undisturbed (fig. S6). We also examined engram cells labeled by a context-only experience (17), and found equivalent engram-cell increases in spine density and synaptic strength (fig. S7) as those labeled by CFC.

DG cells receive information from EC and relay it to area CA3 via the mossy fibers. We labeled DG engram cells using an AAV_9-TRE-ChR2-EYFP virus and simultaneously labeled CA3 engram cells using an AAV_9-TRE-mCherry virus (Fig. 1G). Connection probability was assessed 24 hours post-CFC by stimulating DG $ChR2^+$ cell terminals optogenetically and recording excitatory postsynaptic potentials in CA3 $mCherry^+$ and

mCherry^{-} cells in *ex vivo* preparations. CA3 mCherry^{+} engram cells showed a significantly higher probability of connection than mCherry^{-} cells with DG ChR2^{+} engram cells, demonstrating preferential engram cell to engram cell connectivity. Importantly, this form of engram pathway-specific connectivity was unaffected by post-training administration of ANI (Fig. 1G).

We next tested the behavioral effect of optogenetically stimulating engram cells in amnesic mice (Fig 2A). During CFC training in Context B, both SAL and ANI groups responded to the unconditioned stimuli at equivalent levels (fig. S8). One day post-training, the SAL group displayed robust freezing behavior to the conditioned stimulus of context B, whereas the ANI group showed substantially less freezing behavior (Fig. 2C). Two days post-training, mice were placed into the distinct context A for a 12 min test session consisting of four 3 min epochs of blue light on or off. During this test session, neither group showed freezing behavior during Light-Off epochs, but both froze significantly during Light-On epochs (Fig. 2D). Remarkably, no difference in the levels of light-induced freezing behavior was observed between groups. Three days post-training, the mice were again tested in context B to assay the conditioned response, and retrograde amnesia for the conditioning context was still clearly evident (Fig. 2E). Subjects treated with SAL or ANI following the labeling of a neutral contextual engram (i.e. no shock) did not show freezing behavior in response to light stimulation of engram cells (Fig. 2D). We replicated the DG retrograde amnesia experiment using an alternative widely-used protein synthesis inhibitor, cycloheximide (CHM) (fig. S9). We examined whether ANI administration immediately after CFC altered the activity dependent synthesis of ChR2-EYFP in DG cells and found that this was not the case (Fig. 2F–H). Nevertheless, the dosage of anisomycin used in this study did inhibit protein synthesis in the DG as shown by Arc^{+} cell counting (fig. S10). Thus, the dosage of ANI used was sufficient to induce amnesia, but was insufficient to impair c-fos-tTA driven synthesis of virally delivered ChR2-EYFP in DG cells. Extracellular recordings from SAL and ANI-treated mice confirmed the cell counting results (Fig. 2I–K). In line with fig. S6 and previous reports (24), anisomycin injection 24 hours post-CFC did not cause retrograde amnesia (fig. S11). To provide a negative control for light-induced memory retrieval in amnesia, we disrupted memory encoding by activating hM4Di DREADDs receptors (25) downstream of the DG, in hippocampal CA1, during CFC, and found that subsequent DG engram activation did not elicit memory retrieval (fig. S12).

The recovery from amnesia by direct light activation of ANI-treated DG engram cells was unexpected because these cells showed neither synaptic potentiation nor increased dendritic spine density. We conducted additional behavioral experiments to confirm and characterize the phenomenon. First, we investigated whether recovery from amnesia can be demonstrated by light-induced optogenetic place avoidance test (OptoPA); this would be a measure of an active fear memory recall (see Materials and Methods and (18)), rather than a passive fear response monitored by freezing. SAL and ANI groups displayed equivalent levels of avoidance of the target zone in response to light activation of the DG engram (Fig. 3A). Second, in our previous study we showed that an application of the standard protocol (i.e. 20 Hz) for activation of the CA1 engram was not effective for memory recall (17). However, we found that a 4 Hz protocol applied to the CA1 engram of the SAL and ANI groups elicited similar recovery from amnesia (Fig. 3B). Third, we employed tone fear conditioning (TFC)

and manipulated the fear engram in lateral amygdala (LA) (26) and found light-induced recovery of memory from amnesia. Fourth, we asked whether amnesia caused by disruption of reconsolidation of a contextual fear memory (27–28) can also be recovered by light-activation of DG engram cells, and indeed it was found to be the case (Fig. 3D). We applied the memory inception method (Materials and Methods, (17, 29) to DG engram cells and found that both SAL and ANI groups showed freezing behavior that was specific to the original Context A, demonstrating that light-activated Context A engrams formed in the presence of ANI can function as a CS in a context-specific manner (Fig. 3E). Lastly, we tested the longevity of CFC amnesic engrams for memory recovery by light activation, and found that indeed memory recall could be observed 8 days post-training (fig. S13).

Interactions between the hippocampus and amygdala are crucial for contextual fear memory encoding and retrieval (18). c-Fos expression increases in the hippocampus and amygdala upon exposure of an animal to conditioned stimuli (30–31). These previous observations open up the possibility of obtaining cellular level evidence supporting the behavioral level finding that the recovery from amnesia can be accomplished by direct light activation of ANI-treated DG engram cells. Thus, we compared the effects of natural recall and light-induced recall on amygdala c-Fos$^+$ cell counts in amnesic mice (Fig. 4A–C). c-Fos$^+$ cell counts (Fig. 4B) were significantly lower in basolateral amygdala (BLA) and central amygdala (CeA) of ANI-treated mice compared to SAL mice when natural recall cues were delivered, showing that amygdala activity correlates with fear memory expression (Fig. 4C). In contrast, light-induced activation of the contextual engram cells resulted in equivalent amygdala c-Fos$^+$ counts in SAL and ANI groups (Fig. 4C), supporting the optogenetic behavioral data.

Next, we modified this protocol to include labeling of CA3 and BLA engram cells with mCherry and examined the effects of light-induced activation of DG engram cells on the overlap of mCherry$^+$ engram cells and c-Fos$^+$ recall-activated cells in CA3 and BLA (Fig. 4D). The purpose of this experiment was to investigate whether there is preferential connectivity between the upstream engram cells in DG and the downstream engram cells in CA3 or BLA. Natural recall cues resulted in above chance c-Fos$^+$/mCherry$^+$ overlap in both CA3 and BLA, supporting the physiological connectivity data (Fig. 4E–K). c-Fos$^+$/mCherry$^+$ overlap was significantly reduced in the ANI group compared to the SAL group, but was still higher than chance levels, presumably reflecting incomplete amnesic effects of anisomycin (Fig. 4K). Importantly, light-activation of DG engram cells resulted in equivalent c-Fos$^+$/mCherry overlap as natural cue-induced recall, and this was unaffected by post-CFC anisomycin treatment. These data suggest that there is preferential and protein synthesis-independent functional connectivity between DG and CA3 engram cells, supporting the physiological data (Fig. 1G), and that this connectivity also applies between DG and BLA engram cells.

We previously showed that DG cells activated during CFC training and labeled with ChR2 via the promoter of an immediate early gene (IEG) can evoke a freezing response when they are reactivated optogenetically one to two days later (16), and this has since been achieved in the cortex (21). We have also shown that these DG cells, if light-activated while receiving a US, can serve as a surrogate context-specific CS to create a false CS-US association (17–

18), and that activation of DG or amygdala engram cells can induce place preference (18). Furthermore, recent studies showed that optogenetic inhibition of these cells in DG, CA3, or CA1 impairs expression of a CFC memory (19–20). Together, these findings show that engram cells activated by CFC training are both sufficient and necessary to evoke memory recall, satisfying two crucial attributes in defining a component of a contextual fear memory engram (15). What has been left to be demonstrated, however, is that these DG cells undergo enduring physical changes as an experience is encoded and its memory is consolidated. Although synaptic potentiation has long been suspected as a fundamental mechanism for memory and as a crucial component of the enduring physical changes induced by experience, this has not been directly demonstrated, until the current study, as a property of the engram cells. Our data have directly linked the optogenetically and behaviorally defined memory engram cells to synaptic plasticity.

Based on a large volume of previous studies, (1–3, 7–8, 32–34), a concept has emerged where retrograde amnesia arises from consolidation failure as a result of disrupting the process that converts a fragile memory engram, formed during the encoding phase, into a stable engram with persistently augmented synaptic strength and spine density. Indeed, our current study has demonstrated that amnesic engram cells in the DG one day after CFC training display low levels of synaptic strength and spine density that are indistinguishable from non-engram cells of the same DG. This correlated with a lack of memory recall elicited by contextual cues. Intriguingly, however, direct activation of DG engram cells of the ANI group elicited as much freezing behavior as the activation of these cells of the SAL group. This unexpected finding is supported by a set of additional cellular and behavioral experiments. While amygdala engram cell reactivation upon exposure to the conditioned context is significantly lower in the ANI group compared to the SAL group, optogenetic activation of DG engram cells results in normal reactivation of downstream CA3 and BLA engram cells (Fig. 4). At the behavioral level, the amnesia rescue was observed under a variety of different conditions in which one or more parameters were altered (Fig. 2–3, fig. S9, and fig. S13). Thus, our overall findings indicate that memory engrams survive a post-training administration of protein synthesis inhibitors during the consolidation window and that the memory remains retrievable by ChR2-mediated direct engram activation even after retrograde amnesia is induced. The drive initiated with light-activation of one component of a distributed memory engram (like that in the DG) is sufficient to reactivate engrams in downstream regions (like that in CA3 and BLA) that would also be affected by the systemic injection of a protein synthesis inhibitor (ANI).

Our findings suggest that while a rapid increase of synaptic strength is likely to be crucial during the encoding phase, the augmented synaptic strength is not a crucial component of the stored memory (35–37). This notion is consistent with a recent study showing that an artificial memory could be reversibly disrupted by depression of synaptic strength (38). On the other hand, persistent and specific connectivity of engram cells which we find between DG engram cells and downstream CA3 or BLA engram cells in both SAL and ANI groups may represent a fundamental mechanism of memory information storage (39). These findings also suggest that the primary role of augmented synaptic strength during and after the consolidation phase may be to provide natural recall cues with efficient access to the soma of engram cells for their reactivation and, hence, recall.

The integrative memory engram-based approach employed here for parsing memory and amnesia into encoding, consolidation, and retrieval aspects may be of wider use to other experimental and clinical cases of amnesia, such as Alzheimer's disease (40).

Supplementary Material

Refer to Web version on PubMed Central for supplementary material.

Acknowledgments

We thank X. Liu and B. Roth for sharing reagents; X. Zhou, Y. Wang, W. Yu, S. Huang, and T. O'Connor for technical assistance; J. Z. Young for proofreading; and other members of the Tonegawa Lab for their comments and support. This work was supported by the RIKEN Brain Science Institute, Howard Hughes Medical Institute, and the JPB Foundation (to S.T.).

References

1. Müller GE, Pilzecker A. Z Psychol SI. 1900; 1
2. Duncan CP. J Comp Physiol Psychol. Feb.1949 42:32. [PubMed: 18111554]
3. McGaugh JL. Science. Jan 14.2000 287:248. [PubMed: 10634773]
4. Flexner JB, Flexner LB, Stellar E. Science. Jul 5.1963 141:57. [PubMed: 13945541]
5. Flexner LB, Flexner JB, Roberts RB. Science. Mar 17.1967 155:1377. [PubMed: 6018502]
6. Davis HP, Squire LR. Psychol Bull. Nov.1984 96:518. [PubMed: 6096908]
7. Kandel ER. Science. Nov 2.2001 294:1030. [PubMed: 11691980]
8. Kelleher RJ 3rd, Govindarajan A, Tonegawa S. Neuron. Sep 30.2004 44:59. [PubMed: 15450160]
9. Takeuchi T, Duszkiewicz AJ, Morris RG. Philos Trans R Soc Lond B Biol Sci. Jan 5.2014 369:20130288. [PubMed: 24298167]
10. Govindarajan A, Israely I, Huang SY, Tonegawa S. Neuron. Jan 13.2011 69:132. [PubMed: 21220104]
11. Krug M, Lossner B, Ott T. Brain Res Bull. Jul.1984 13:39. [PubMed: 6089972]
12. Frey U, Krug M, Reymann KG, Matthies H. Brain Res. Jun 14.1988 452:57. [PubMed: 3401749]
13. Huang YY, Nguyen PV, Abel T, Kandel ER. Learn Mem. Sep-Oct;1996 3:74. [PubMed: 10456078]
14. Semon, R. Die Mneme als erhaltendes Prinzip im Wechsel des organischen Geschehens. Wilhelm Engelmann; Leipzig: 1904.
15. Josselyn SA. J Psychiatry Neurosci. Jul.2010 35:221. [PubMed: 20569648]
16. Liu X, et al. Nature. Apr 19.2012 484:381. [PubMed: 22441246]
17. Ramirez S, et al. Science. Jul 26.2013 341:387. [PubMed: 23888038]
18. Redondo RL, et al. Nature. Sep 18.2014 513:426. [PubMed: 25162525]
19. Denny CA, et al. Neuron. Jul 2.2014 83:189. [PubMed: 24991962]
20. Tanaka KZ, et al. Neuron. Oct 8.2014
21. Cowansage KK, et al. Neuron. Oct 8.2014
22. Reijmers LG, Perkins BL, Matsuo N, Mayford M. Science. Aug 31.2007 317:1230. [PubMed: 17761885]
23. Clem RL, Huganir RL. Science. Nov 19.2010 330:1108. [PubMed: 21030604]
24. Suzuki A, et al. J Neurosci. May 19.2004 24:4787. [PubMed: 15152039]
25. Armbruster BN, Li X, Pausch MH, Herlitze S, Roth BL. Proc Natl Acad Sci U S A. Mar 20.2007 104:5163. [PubMed: 17360345]
26. Han JH, et al. Science. Mar 13.2009 323:1492. [PubMed: 19286560]
27. Misanin JR, Miller RR, Lewis DJ. Science. May 3.1968 160:554. [PubMed: 5689415]
28. Nader K, Schafe GE, Le Doux JE. Nature. Aug 17.2000 406:722. [PubMed: 10963596]

29. Liu X, Ramirez S, Tonegawa S. Philos Trans R Soc Lond B Biol Sci. 2014; 369:20130142. [PubMed: 24298144]
30. Besnard A, Laroche S, Caboche J. Brain Struct Funct. Jan.2014 219:415. [PubMed: 23389809]
31. Hall J, Thomas KL, Everitt BJ. Eur J Neurosci. Apr.2001 13:1453. [PubMed: 11298807]
32. McGaugh JL. Science. Sep 16.1966 153:1351. [PubMed: 5917768]
33. Dudai Y. Annu Rev Psychol. 2004; 55:51. [PubMed: 14744210]
34. Johansen JP, Cain CK, Ostroff LE, LeDoux JE. Cell. Oct 28.2011 147:509. [PubMed: 22036561]
35. Miller RR, Matzel LD. Learn Mem. Sep-Oct;2006 13:491. [PubMed: 17015845]
36. Miller CA, Sweatt JD. Learn Mem. Sep-Oct;2006 13:498. [PubMed: 17015846]
37. Chen S, et al. Elife. Nov 17.2014 3
38. Nabavi S, et al. Nature. Jul 17.2014 511:348. [PubMed: 24896183]
39. Hebb, DO. The organization of behavior; a neuropsychological theory. Wiley; New York: 1949.
40. Daumas S, et al. Learn Mem. Sep.2008 15:625. [PubMed: 18772249]
41. Boyden ES, Zhang F, Bamberg E, Nagel G, Deisseroth K. Nat Neurosci. Sep.2005 8:1263. [PubMed: 16116447]

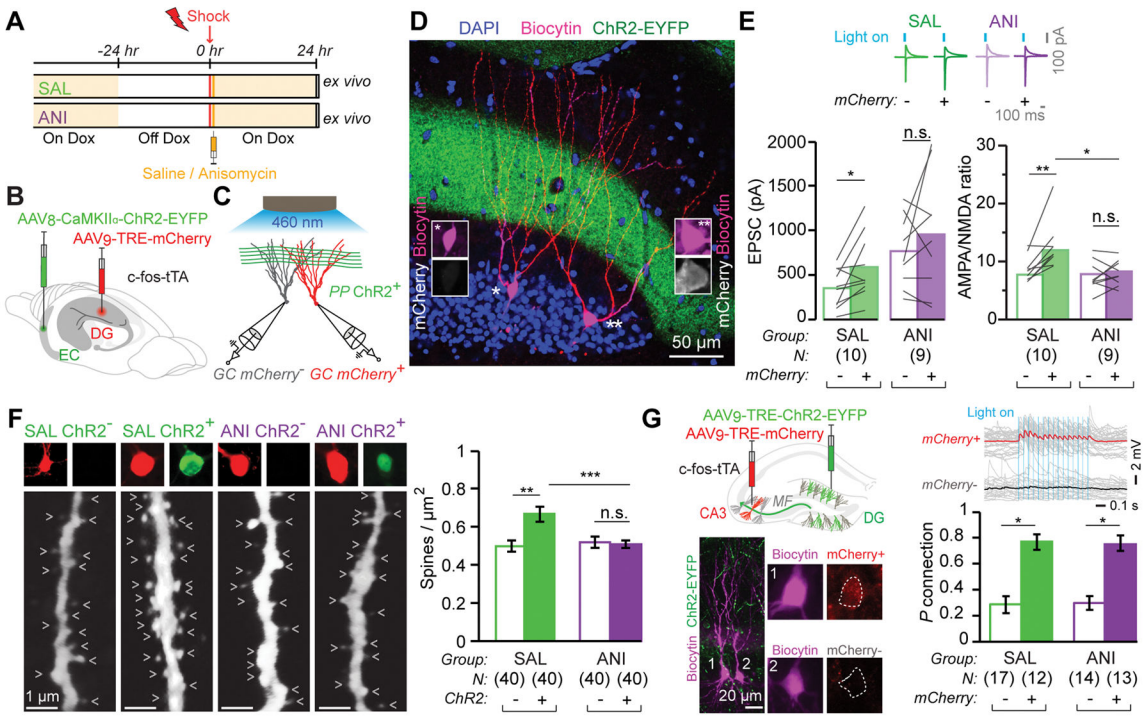

Figure 1. Synaptic Plasticity and Connectivity of Engram Cells

(A) Mice taken Off DOX 24 hrs before contextual fear conditioning (CFC) and dispatched 24 hrs post training. Saline (SAL) or anisomycin (ANI) administered immediately after training.

(B) AAV_8-CaMKIIα-ChR2-EYFP and AAV_9-TRE-mCherry viruses injected into the entorhinal cortex and dentate gyrus, respectively, of c-fos-tTA mice.

(C) Paired recordings of engram (red) and non-engram (grey) DG cells during optogenetic stimulation of $ChR2^+$ perforant path (PP) axons.

(D) Representative image of a pair of recorded biocytin-labeled engram ($mCherry^+$) and non-engram ($mCherry^-$) DG cells. Note $ChR2^+$ PP axons in green.

(E) (Top) Example traces of AMPA and NMDA receptor-dependent postsynaptic currents in $mCherry^+$ and $mCherry^-$ cells, evoked by light activation of $ChR2^+$ PP axons. (Bottom) EPSC amplitudes and AMPA/NMDA current ratios of $mCherry^+$ and $mCherry^-$ cells of the two groups are displayed as means (columns) and individual paired data points (grey lines). Paired t-test * $p < 0.05$, ** $p < 0.001$. SAL group compared with the ANI group, unpaired t-test * $p < 0.05$.

(F) (Left) Representative confocal images of biocytin filled dendritic fragments derived from SAL and ANI groups for $ChR2^+$ and $ChR2^-$ cells (arrow heads: dendritic spines). (Right) Average dendritic spine density showing an increase occurring exclusively in $ChR2^+$ fragments. Data are represented as mean ± SEM. Unpaired t tests ** $p < 0.01$, *** $p < 0.001$.

(G) Engram Connectivity. (Top left) AAV_9-TRE-ChR2-EYFP and AAV_9-TRE-mCherry viruses, injected into the DG and CA3, respectively, of c-fos-tTA mice. (Bottom left) Example of $mCherry^+$ (1) and $mCherry^-$ (2) biocytin-filled CA3 pyramidal cells. Note $ChR2^+$ mossy fibers (MF) in green. (Top Right) $mCherry^+$ cell but not $mCherry^-$ cell

displayed EPSPs in response to optogenetic stimulation of MF. (Bottom Right) Probability of connection of DG ChR2^{+} engram axons and CA3 mCherry^{+} and mCherry^{-} cells. Error bars are approximated by binomial distribution. Fisher's exact test: * $p < 0.05$.

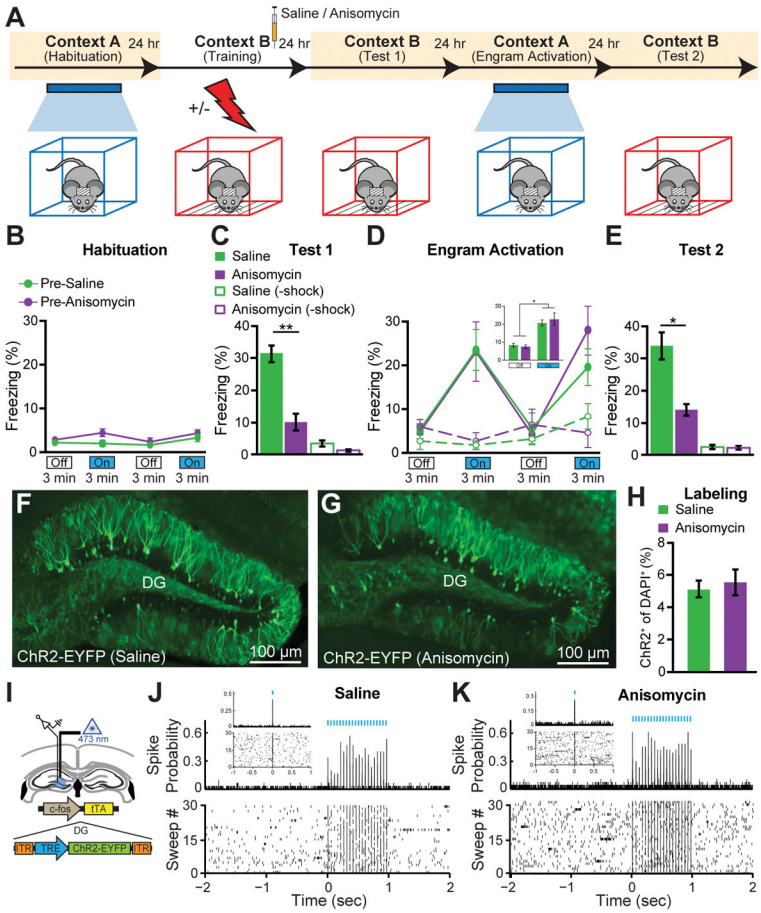

Figure 2. Optogenetic Stimulation of DG Engram Cells Restores Fear Memory in Retrograde Amnesia

(A) Behavioral schedule. Beige shading signifies that subjects are On DOX, precluding ChR2 expression. Mice taken off DOX 24–30 hrs before CFC in Context B. SAL or ANI was injected into the mice after training.

(B) Habituation to Context A with Light-Off and Light-On epochs. Blue light stimulation of the DG did not cause freezing behavior in naïve, unlabelled mice of the pre-SAL (n = 10) or pre-ANI (n = 8) groups.

(C) Memory recall in Context B 1 day post-training (Test 1). ANI group displayed significantly less freezing than SAL group ($p < 0.005$). No-shock groups with SAL (n = 4) or ANI (n = 4) did not display freezing upon re-exposure to Context B.

(D) Memory recall in Context A 2 days post-training (Engram Activation) with Light-Off and Light-On epochs. Freezing for the two Light-Off and Light-On epochs are further averaged in the inset. Significant freezing due to light stimulation was observed in both the SAL ($p < 0.01$) and ANI groups ($p < 0.05$). Freezing levels did not differ between groups. SAL and ANI-treated no-shock control groups did not freeze in response to light stimulation of context B engram cells.

(E) Memory recall in Context B 3 days post-training (Test 2). ANI group displayed significantly less freezing than SAL group ($p < 0.05$).

(F, G) Images showing DG sections from c-fos-tTA mice 24 hrs after SAL or ANI treatment.

(H) ChR2-EYFP cell counts from DG sections of SAL (n = 3) and ANI (n = 4) groups.
(I) *In vivo* anesthetized recordings (see Materials and Methods).
(J, K) Light pulses induced spikes in DG neurons recorded from head-fixed anesthetized c-fos-tTA mice 24 hrs after treatment with either SAL or ANI.
Data presented as mean ± SEM.

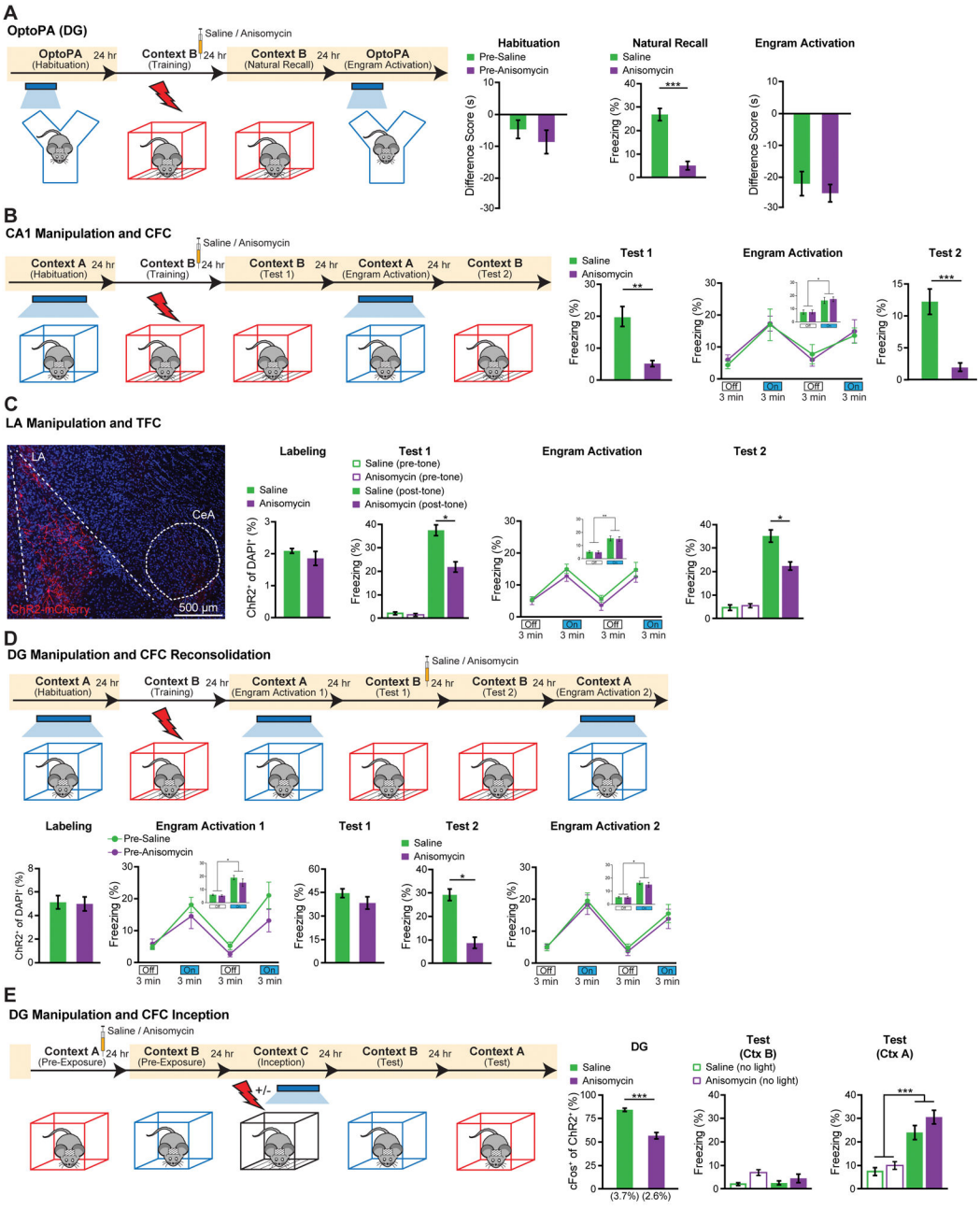

Figure 3. Recovery of Memory from Amnesia under a Variety of Conditions

(A) DG engram activation and optogenetic place avoidance (OptoPA). During habituation neither group displayed significant avoidance of target zone. For Natural Recall the ANI group (n = 10) displayed significantly less freezing than SAL group (n = 12) in Context B ($p < 0.005$). SAL and ANI displayed similar levels of OptoPA.

(B) CA1 engram activation and CFC. 1 day post-CFC (Test 1) ANI group (n = 9) displayed significantly less freezing than SAL group (n = 10) in Context B ($p < 0.01$). 2 days post-training (Engram Activation), light-activation of CA1 engrams elicited freezing in both SAL

($p < 0.01$) and ANI groups ($p < 0.001$). 3 days post-training (Test 2) ANI group froze less than SAL group in Context B ($p < 0.01$).

(C) Lateral amygdala (LA) engram activation and tone fear conditioning (TFC). The behavioral schedule was identical to that in Fig. 3B, except that context tests were replaced with tone tests in Context C (Materials and Methods). (Left) example image of ChR2-mCherry labeling of LA neurons. 2% of DAPI cells were labeled by ChR2. (Right) 1 day post-training (Test 1), ANI group ($n = 9$) displayed significantly less freezing to tone than SAL group ($n = 9$) ($p < 0.05$). 2 days post-training (Engram Activation), significant light-induced freezing was observed for both SAL ($p < 0.005$) and ANI groups ($p < 0.005$). 3 days post-training (Test 2) ANI group froze less to tone than SAL group ($p < 0.05$).

(D) DG engram activation and CFC reconsolidation. ANI ($n = 11$) and SAL ($n = 11$) groups showed similar levels of ChR2 labeling. Both groups showed light-induced freezing behavior 1 day post-training (Engram Activation 1), pre-SAL ($P < 0.001$), pre-ANI ($P < 0.02$). 2 days post training, (Test 1) the fear memory was reactivated by exposure to Context B, and SAL or ANI injected. 3 days post-training, (Test 2) the ANI group froze significantly less than SAL to Context B ($p < 0.01$). 4 days post-training, (Engram Activation 2) significant light-induced freezing was observed for the SAL ($p < 0.001$) and ANI ($p < 0.003$) groups.

(E) DG Inception (Materials and Methods) following contextual memory amnesia. Context-only engram was labeled for target Context A, followed by injection of SAL ($n = 11$) or ANI ($n = 11$). Amnesia demonstrated in ANI group by decreased $ChR2^{+}$/c-Fos^{+} co-labeling following Context A re-exposure 1 day post labeling.

Following fear inception, neither SAL nor ANI groups displayed freezing behavior in Context B, while both groups displayed significant freezing in Context A, with no significant difference between groups. No-light inception SAL ($n = 7$) and ANI ($n = 6$) controls displayed no freezing to Context A or B. Statistical comparison are performed by using unpaired t tests, *** $p < 0.001$.

Data presented as mean ± SEM.

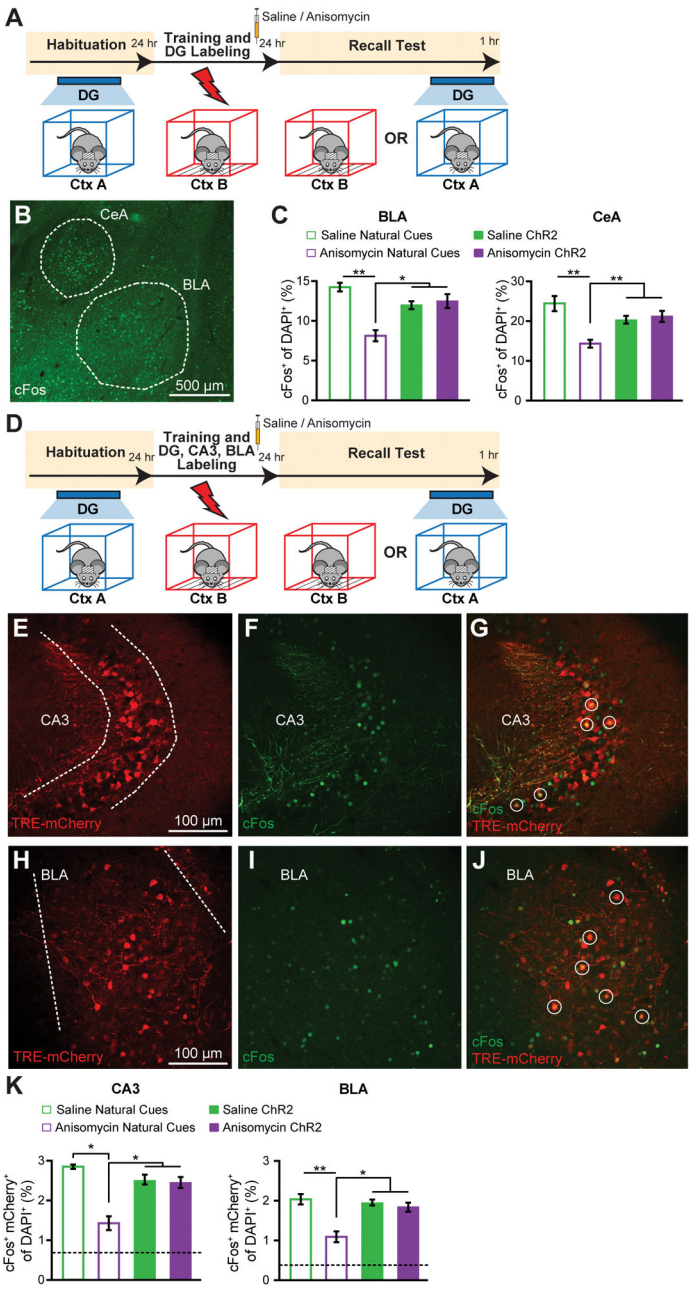

Figure 4. Amygdala Activation and Functional Connectivity in Amnesia by Light Activation of DG Engram

(A) Schedule for cell counting experiments. Mice were either given a natural recall session in Context B, or a light-induced recall session in Context A. Mice were perfused 1 hr post recall.

(B) Representative image showing c-Fos expression in the basolateral amygdala (BLA) and central amygdala (CeA).(C) c-Fos$^+$ cell counts in the BLA and CeA of mice following natural or light-induced recall (n = 3–4 per group).

(D) Schedule for cell counting experiments. c-fos-tTA mice with AAV$_9$-TRE-ChR2-EYFP injected into the DG and AAV$_9$-TRE-mCherry injected into both CA3 and BLA were fear

conditioned off DOX, and 1 day later were given a natural recall session in Context B, or a light-induced recall session in Context A. Mice were perfused 1 hr post recall.

(E – G) Representative images showing mCherry engram cell labeling, c-Fos expression, $mCherry^{+}/c\text{-}Fos^{+}$ overlap in CA3.

(H – J) Representative images showing mCherry engram cell labeling, c-Fos expression, mCherry/c-Fos overlap in BLA.

(K) $c\text{-}Fos^{+}/mCherry^{+}$ overlap cell counts in CA3 and BLA of mice following natural or light-induced recall (n = 3 – 4 per group). Chance levels were estimated at 0.76 (CA3) and 0.42 (BLA). Data are presented as mean ± SEM. Statistical comparison are performed by using unpaired t tests, * $p < 0.05$, ** $p < 0.01$.